



COLLECTIVE-MODE ac CONDUCTION IN THE BLUE BRONZE $K_{0.3}MoO_3$

R. P. Hall, M. S. Sherwin and A. Zettl

Department of Physics, University of California, Berkeley
Berkeley, CA 94720, USA

(Received 17 January 1985 by A. Zawadowski)

We have measured the low field ac conductivity of the blue bronze $K_{0.3}MoO_3$ in the charge density wave (CDW) state, over the frequency range 10 Hz to 2.4 GHz. At selected temperatures and over an extended frequency range, our results are consistent with the model of low frequency CDW relaxation, proposed by Cava *et al.* However, there is apparent at high frequencies an additional relaxation mechanism. Characteristic crossover frequencies and energies associated with this high frequency dynamic mode appear similar to those obtained previously for $NbSe_3$ and TaS_3 . Our results suggest at least two distinct CDW relaxation processes in $K_{0.3}MoO_3$.

The blue bronze $K_{0.3}MoO_3$ is representative of a new class of materials which display charge density wave (CDW) transport. Although it has been known for some time that $K_{0.3}MoO_3$ undergoes a metal-to-insulator phase transition¹, the anomalous transport properties of the insulating state have only recently been associated with CDW formation and dynamics. Below the Peierls transition temperature $T_p = 180$ K, nonlinear dc conduction is observed in $K_{0.3}MoO_3$ after a sharp threshold electric field is exceeded.² The excess dc conductivity is associated with a depinning and subsequent Fröhlich-type motion of the CDW condensate. In many samples of $K_{0.3}MoO_3$, the onset of CDW conduction is accompanied by hysteretic switching, and broad-band and narrow-band noise.² Such features were first observed in the prototype CDW conductor $NbSe_3$, and appear to be general trademarks of CDW depinning.

A very interesting feature of CDW dynamics concerns not the dc conduction, but rather the ac response of the pinned mode. Random impurities may pin the phase of the CDW condensate, either at the impurity, as in strong impurity pinning, or over a spatially finite region, as in weak impurity pinning. In these cases the oscillator strength of the CDW response is moved to finite frequency, inhibiting Fröhlich superconductivity.³ The characteristic response frequencies for the pinned mode may be orders of magnitude smaller than those associated with single-particle excitations across the Peierls semiconducting gap. For $NbSe_3$ and TaS_3 , typical "crossover" frequencies for the ac response are in the range 50 MHz to 500 MHz, depending on sample purity.^{4,5} We identify the crossover frequency as that frequency for which the ac conductivity reaches one half its maximum value.

The relative ease with which the CDW in $K_{0.3}MoO_3$ may be depinned by dc electric fields (for pure samples, $E_T \approx 100$ mV/cm at 100 K) suggests, as with $NbSe_3$ and TaS_3 , rather low pinning energies. Consequently, anomalous ac response might be expected at relatively low frequencies.

Recently, two ac conductivity studies of $K_{0.3}MoO_3$ were undertaken to investigate this possibility. Cava *et al.*⁶ have identified an anomalous temperature-dependent response in the frequency range 5 Hz to 13 MHz. For example, at $T = 60$ K, the entire oscillator strength for the pinned condensate was identified to be below 10 MHz, an exceptionally low frequency range. On the other hand, Travaglini and Wachter⁷ recently performed optical studies on $K_{0.3}MoO_3$. At $T = 5$ K anomalous ac response appeared between 0.4 meV (97 GHz) and 7 meV (1680 GHz). Here the pinned mode was identified to be centered on 1.8 meV (432 GHz), independent of temperature.

We here attempt to clarify the ac response parameters of the CDW condensate in $K_{0.3}MoO_3$. We have performed careful low-field ac conductivity measurements in the frequency range 10 Hz to 2.3 GHz. We find that the characteristic response parameters of $K_{0.3}MoO_3$ in the low microwave regime are similar to those intrinsic to $NbSe_3$ and TaS_3 . We suggest that the additional structure observed at very low (audio) and very high (infrared) frequencies, although associated with the CDW condensate, do not reflect by themselves the full CDW oscillator strength.

We have prepared single crystals of $K_{0.3}MoO_3$ by electrochemical growth. Starting materials of K_2MoO_4 and MoO_3 were combined in a molar ratio of 1:3.15, ground to a fine powder, and fused at 600°C for 5 hours. Following slow cooling, the resultant mixture was reground and heated to 500°C. Crystal growth was initiated by platinum electrodes immersed in the melt, with a bias current of 40 mA. A total reaction time of 24 hours yielded single crystals of $K_{0.3}MoO_3$ of varied size, the largest being typically 5 mm x 7 mm x 3 mm, and the smallest of submillimeter dimension. Typical dimensions for crystals used in this study were 1 mm x 0.2 mm x 0.1 mm, with the long dimension corresponding to the highly conducting (b) axis. All measurements reported here are with respect to this axis. Electrical contact to the

samples was made by evaporated indium pads covered with conductive silver paint.

Two different methods were used to determine the complex ac conductivity $\sigma(\omega)$ for $K_{0.3}MoO_3$. In the frequency range 10 Hz to 10 MHz, a computer-controlled impedance bridge was employed. This method allowed both 2-probe and 4-probe sample mounting configurations, and data was obtained as a continuous function of frequency. Typically, at a fixed temperature, ten frequency sweeps were recorded and signal averaged by computer to yield reliable data. No significant differences were found between 2-probe and 4-probe measurements, indicating negligible contact impedances. In the frequency range 4 MHz to 2.3 GHz, an automatic network analyzer (HP 8754A) was used. Again, frequency sweeping was continuous, but a 2-probe sample mounting configuration was used exclusively. For both measurement methods, the ac drive level was fixed at approximately 1 mV rms, and provisions existed for simultaneous measurement of the dc conductivity.

Figure 1 shows, for a single $K_{0.3}MoO_3$ crystal, the low field conductivity measured as a function of temperature at dc and 2.3 GHz. The dc conductivity is consistent with that obtained in previous studies,¹ showing a metal-insulator transition at $T_p = 180$ K. At temperatures below T_p , $\sigma(dc)$ follows an approximately activated semiconducting behavior, and from $\sigma(dc) = A \exp(-2\Delta/2kT)$, we find $2\Delta = 860$ K at 100 K. This identifies the Peierls gap. In the temperature region above T_p , within experimental error, $\sigma(dc) = \sigma(2.3 \text{ GHz})$, indicating no frequency dependence to the conductivity. This is expected for a metal at these relatively low frequencies. Below T_p , however, the 2.3 GHz conductivity is substantially larger than the dc value, and at

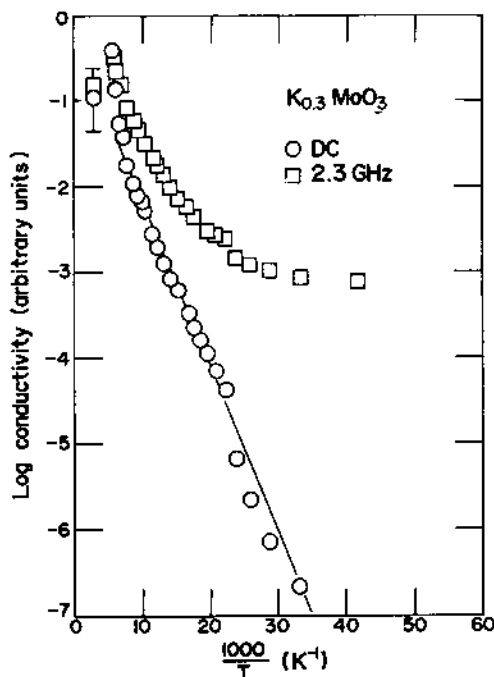


Fig. 1 Low-field conductivity of blue bronze $K_{0.3}MoO_3$ measured at dc and 2.4 GHz. The solid line represents an activated behaviour with $2\Delta = 860$ K.

$T = 42$ K the ac conductivity is enhanced by nearly three orders of magnitude. Hence a strong frequency-dependent response is observed at frequencies nearly 4 orders of magnitude smaller than the single-particle gap 2Δ .

Figure 2 shows, at selected temperatures, the frequency dependent response in greater detail. This data represents three samples chosen from the same preparation batch, with comparable dimensions and dc threshold electric fields ($E_T \approx 500$ mV/cm at $T = 100$ K). Because of slight variations in sample dimensions (and hence absolute conductivity) all data has been normalized to the dc conductivity measured at room temperature. Between 10 Hz and 2.3 GHz, both the real and imaginary parts of the ac conductivity, $\text{Re } \sigma(\omega)$ and $\text{Im } \sigma(\omega)$, increase in a smooth and continuous manner, with no evidence for a threshold frequency for the onset of ac CDW conduction. Because of the impedance limits of our measuring instruments, we were not able to extend the measurements to temperatures lower than approximately 40 K.

Although the overall frequency dependence of $\sigma(\omega)$ in $K_{0.3}MoO_3$ resembles that observed in $NbSe_3$ and TaS_3 , there are notable differences. The most striking is an anomalous low frequency behavior, reported previously by Cava et al.⁶ The low frequency anomalies appearing in our samples are shown more clearly in figure 3a. This figure shows the CDW contribution to the ac response, $\text{Re } \sigma_{CDW}(\omega)$ and $\text{Im } \sigma_{CDW}(\omega)$, for $K_{0.3}MoO_3$ in the frequency range 10 kHz to 2.3 GHz, at temperature $T = 77$ K. This plot was obtained from the data of figure 2 by numerically subtracting the dc contribution of normal electrons. As indicated by the error bars on the figure, such a subtraction leads to a large uncertainty in the reduced data, especially at low frequency.

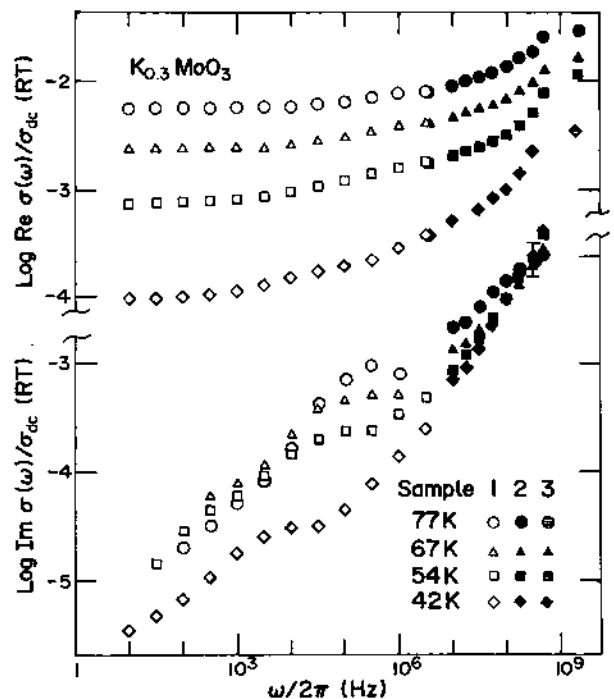


Fig. 2 Real and Imaginary components of low-field ac conductivity of $K_{0.3}MoO_3$, at selected temperatures in the CDW state.

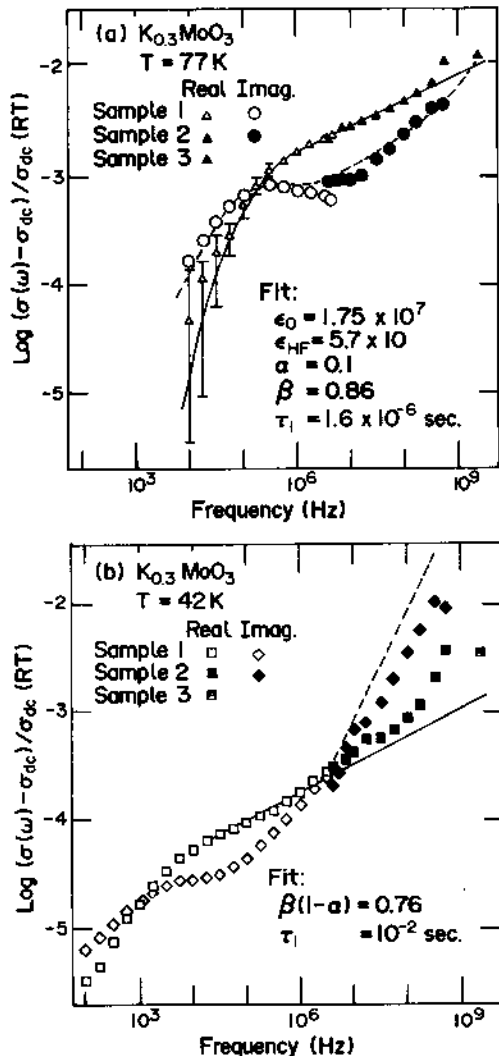


Fig. 3 a) CDW contribution to ac response of $K_{0.3}MoO_3$ at 77 K. The solid and dashed lines are fits to Eq. (2), with parameters given on the figure. b) CDW contribution to ac response of $K_{0.3}MoO_3$ at 42 K. The solid and dashed lines are fits to Eq. (2), with parameters given on the figure. The high frequency response is not well described by Eq. (2).

Cava *et al.* have analyzed the low frequency anomaly in terms of a general dielectric function⁶

$$\epsilon(\omega) = \epsilon_{HF} + (\epsilon_0 - \epsilon_{HF}) \frac{1}{[1 + (i\omega\tau_1)^{1-\alpha}]^\beta} \quad (1)$$

with

$$\sigma_{CDW}(\omega) = i\omega\epsilon(\omega) \quad (2)$$

ϵ_{HF} represents the high frequency dielectric constant, ϵ_0 the static dielectric constant, and τ_1 a characteristic relaxation time. Eq. (1) actually incorporates a distribution of relaxation times, with the (temperature dependent) parameters α and β characters respectively the width and skewness of the distribution. Eq. (2) gives the complex conductivity as a complicated

function of the applied frequency ω . However, in various limits, Eq. (2) may be simplified. At low frequencies ($\omega\tau_1 \ll 1$),

$$\text{Re } \sigma_{CDW}(\omega) \sim \epsilon_0(\omega\tau_1)^{2-\alpha}, \quad \text{and} \quad (3a)$$

$$\text{Im } \sigma_{CDW}(\omega) \sim \epsilon_0(\omega\tau_1)^{1.0} \quad (3b)$$

With a small $\text{Im } \sigma_{CDW}(\omega)$ will dominate $\text{Re } \sigma_{CDW}(\omega)$. At high frequencies ($\omega\tau_1 \gg 1$), Eq. (2) reduces to

$$\text{Re } \sigma_{CDW}(\omega) \sim \epsilon_0(\omega\tau_1)^{1-\beta(1-\alpha)}, \quad \text{and} \quad (4a)$$

$$\text{Im } \sigma_{CDW}(\omega) \sim \epsilon_{HF}(\omega\tau_1)^{1.0} + \frac{\epsilon_0(\omega\tau_1)^{1-\beta(1-\alpha)}}{\sin[\frac{\pi}{2}(1-\alpha)]} \quad (4b)$$

With $1-\beta(1-\alpha)$ between 0.2 and 0.3 (see Ref. 6), $\text{Im } \sigma_{CDW}(\omega)$ dominates $\text{Re } \sigma_{CDW}(\omega)$. However, at intermediate frequencies (near $\omega = \tau_1^{-1}$), $\text{Re } \sigma_{CDW}(\omega)$ dominates $\text{Im } \sigma_{CDW}(\omega)$. Eq. (2) thus predicts, over an extended frequency range, two points crossings of $\text{Re } \sigma_{CDW}(\omega)$ and $\text{Im } \sigma_{CDW}(\omega)$.

In fig. 3a, Eqns. (1) and (2) have been fit to the experimental data at $T = 77$ K, with fitting parameters identified on the figure. We note that the characteristic relaxation time $\tau_1 = 1.6 \mu$ sec corresponds to an unusually low characteristic frequency, $\omega_1 = 3.9$ MHz. This value is in general agreement with the results of Cava *et al.*, and is substantially lower than characteristic frequencies observed in $NbSe_3$ and TaS_3 . Although only one point crossing of $\text{Re } \sigma_{CDW}(\omega)$ and $\text{Im } \sigma_{CDW}(\omega)$ is observed in the data of fig. 3a, the data are not inconsistent with such a possibility at frequencies slightly higher than we have measured. In general, Eq. (1) appears to provide a good fit to our $\sigma_{CDW}(\omega)$ data at $T = 77$ K.

With decreasing temperature below 77 K, the data of fig. 2 indicates, in terms of Eq. (1), a smooth decrease in the characteristic frequency ω_1 . Fig. 3b shows in detail $\text{Re } \sigma_{CDW}(\omega)$ and $\text{Im } \sigma_{CDW}(\omega)$ for $K_{0.3}MoO_3$ at 42 K. Here two point crossings of $\text{Re } \sigma_{CDW}(\omega)$ and $\text{Im } \sigma_{CDW}(\omega)$ are indeed observed, and a detailed fit to Eq. (1) indicates $\tau_1 = 10$ ms, which corresponds to a characteristic frequency $\omega_1 = 628$ Hz. However, there are clear departures from Eq. (1) in the 42 K data, especially at high frequency. The solid and dashed lines in fig. 3b are respectively $\text{Re } \sigma_{CDW}(\omega)$ and $\text{Im } \sigma_{CDW}(\omega)$, as calculated from Eq. (1). The fitting parameters identified on the figure have been obtained from analysis of the low ($\omega/2\pi < 1$ MHz) frequency data. Above approximately 1 MHz, $\text{Re } \sigma_{CDW}(\omega)$ increases more rapidly than Eq. (1) would predict, while $\text{Im } \sigma_{CDW}(\omega)$ increases less rapidly. Preliminary work on $K_{0.3}MoO_3$ at microwave frequencies⁸ suggests that $\text{Re } \sigma_{CDW}(\omega)$ and $\text{Im } \sigma_{CDW}(\omega)$ continue to increase with increasing frequency below 10 GHz, in a manner consistent with our experimental data. Thus Eqns. (1) and (2), while providing excellent fits to the very low frequency data, are in strong disagreement with the experimentally determined high frequency conductivity of $K_{0.3}MoO_3$.

We interpret the strong increase in the ac conductivity at high frequency in $K_{0.3}MoO_3$ as due to the collective ac response of the pinned CDW mode. At sufficiently high frequencies, it is expected that $\text{Re } \sigma_{CDW}(\omega)$ will saturate (and

eventually turn over with increasing frequency), while $\text{Im } \sigma_{CDW}(\omega)$ should display an inflection. Such a behaviour is in fact mandated by the conductivity sum rule. As a saturation of $\text{Re } \sigma_{CDW}$ or turn over in $\text{Im } \sigma_{CDW}$ is not evident in fig. 3b, the characteristic frequency associated with this "second" CDW relaxation process, ω_2 , is necessarily greater than approximately 2 GHz.

The additional high frequency response apparent in fig. 3b is present at all temperatures in the CDW state, not only near 42 K. However, with increasing temperature above 42 K, the effect of the high frequency relaxation becomes masked to a larger and larger degree by the (temperature-dependent) low frequency (τ_1) relaxation process, which forms a substantial contribution to the total CDW ac response between 10 Hz and 100 MHz at 77 K.

We now consider the high frequency (ω_2) relaxation process in detail. It appears somewhat analogous to the conventional CDW ac response observed previously in $NbSe_3$ (Ref. 4) and TaS_3 (Ref. 5). In both these materials, the overall behaviour of $\sigma_{CDW}(\omega)$ is described in a crude way by an overdamped-harmonic oscillator solution,⁹

$$\text{Re } \sigma_{CDW}(\omega) = \sigma_0 [1 + (\omega_{CO}/\omega)^2]^{-1} \quad (5a)$$

$$\text{Im } \sigma_{CDW}(\omega) = \sigma_0 \frac{\omega_{CO}}{\omega} [1 + (\omega_{CO}/\omega)^2]^{-1} \quad (5b)$$

with σ_0 representing the peak value of $\text{Re } \sigma_{CDW}$, and ω_{CO} the classical crossover frequency. In the overdamped case, we identify ω_{CO} with ω_2 . Eqns. (5a) and (5b) reflect a special case of the generalized Debye dielectric constant, Eq. (1), with a zero high frequency contribution, and delta function distribution for relaxation times.

Fig. 4 shows the normalized high frequency response of $K_{0.3}MoO_3$ at $T = 42$ K, along with the

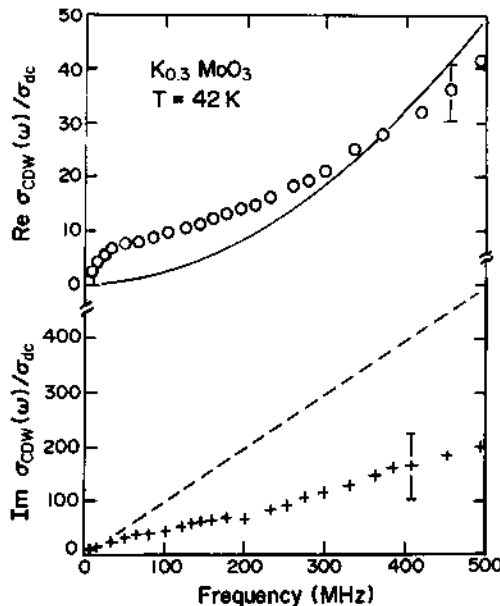


Fig. 4 Normalized high frequency ac conductivity of $K_{0.3}MoO_3$ at $T = 42$ K. The solid and dashed lines are fits to Eqns. (5a) and (5b), respectively, with parameters given in the text.

predictions of Eq. (5) with chosen parameters $\sigma_0 = 5 \times 10^3 \sigma(\text{dc})$ and $\omega_{CO} = 5$ GHz. We here compare Eq. (5) to only the low temperature data, in order to avoid a tortuous convolution with the low frequency (τ_1) relaxation process, not contained in Eq. (5). It is apparent from fig. 4 that the high frequency conductivity in $K_{0.3}MoO_3$ is not well described by a simple harmonic oscillator solution (we note that a similarly poor fit is obtained from Bardeen's tunneling formula¹⁰). However, a best fit of Eq. (5) yields characteristic timescales consistent with those extracted from the trichalcogenides $NbSe_3$ and TaS_3 , and also in reasonable agreement with the dc threshold field of $K_{0.3}MoO_3$.¹¹ A better fit to the data in fig. 4 may be obtained by invoking a distribution in relaxation times (Eq. (1)); the characteristic frequency obtained from such a fit however remains consistent with a cross-over frequency near 5 GHz. Between approximately 1 MHz and 100 MHz, $\text{Re } \sigma_{CDW}(\omega)$ and $\text{Im } \sigma_{CDW}(\omega)$ in $K_{0.3}MoO_3$ are well described by power law behaviour. For example, at $T = 42$ K, the high frequency data of fig. 3b indicate $\text{Re } \sigma \sim \omega^{0.5}$ and $\text{Im } \sigma \sim \omega^{0.7}$. These exponents are nearly identical to those which describe the complex ac conductivity of orthorhombic TaS_3 between 30 MHz and 1 GHz, at $T = 90$ K.¹² Power law behaviour in TaS_3 (at somewhat higher temperature) has been discussed in detail by Wu et al.¹³ in terms of relaxational dynamics of the CDW condensate.

Our conductivity measurements on $K_{0.3}MoO_3$ suggest that a substantial portion of the CDW oscillator strength will be found in the frequency range 1 MHz to 50 GHz, the upper limit being a rough estimate. It is interesting to speculate on the significance of the low frequency (audio) and very high frequency (infrared) conductivity anomalies. In considering the low frequency anomaly first reported by Cava et al.,⁶ we note that the CDW in $K_{0.3}MoO_3$ appears to smoothly approach commensurability with the underlying lattice at temperatures below 100 K.¹⁴ One possibility for low frequency response is thus solitons, where the movement of phase dislocations is energetically favored over bulk oscillation of the CDW condensate at low frequency. Another (perhaps related) possibility is that the low frequency ac conductivity reflects changes in the metastable states of the crystal. Detailed studies of the dc^{2,15} and ac¹⁶ response parameters of $K_{0.3}MoO_3$ have indicated an extraordinarily rich metastable state structure, with characteristic lifetimes of a particular metastable state often in the millisecond range, corresponding to audio response in the frequency domain. The infrared peak discussed by Travaglini and Wachter⁷ clearly is associated with an electronic response. However, this could result not from the collective CDW excitation, but rather from coupling between the CDW and phonons, resulting in a phonon mode peak. At present, it appears difficult to clearly define the relation between the infrared anomaly and the CDW phase mode. We remark that the CDW amplitude mode has been previously identified by Raman studies.¹⁷

In summary, we have measured the low-field complex ac conductivity of $K_{0.3}MoO_3$ between 10 Hz and 2.4 GHz. In addition to the low frequency anomalies reported previously, we find anomalous conduction at higher frequencies, characteristic of pinned CDW response in the microwave regime.

It thus appears that there exist at least two distinct (and relatively complex) relaxation processes in the CDW state of $K_{0.3}MoO_3$.

Acknowledgement - We thank R. M. Fleming, P. Littlewood, and L. Mihaly for useful discussions. This research was supported by NSF grant DMR 8400041. One of us (A.Z.) is an Alfred P. Sloan Foundation Fellow.

REFERENCES

1. W. Fogle and J. H. Perlstein, *Phys. Rev.* **B6**, 1402 (1972).
2. J. Dumas, C. Schlenker, J. Marcus, and R. Buder, *Phys. Rev. Lett.* **50**, 757 (1983).
3. P. A. Lee, T. M. Rice, and P. W. Anderson, *Solid State Commun.* **14**, 703 (1974).
4. G. Grüner, L. C. Tippie, J. Sanny, W. G. Clark, and N. P. Ong, *Phys. Rev. Lett.* **45**, 935 (1980); A. Zettl and G. Grüner, *Phys. Rev.* **B29**, 755 (1984).
5. A. Zettl and G. Grüner, *Phys. Rev.* **B25**, 2081 (1982); A. Zettl, C. M. Jackson, and G. Grüner, *Phys. Rev.* **B26**, 5773 (1982).
6. R. J. Cava, R. M. Fleming, P. Littlewood, E. A. Rietman, L. F. Schneemeyer, and R. G. Dunn, *Phys. Rev.* **B30**, 3228 (1984).
7. G. Travaglini and P. Wachter, *Phys. Rev.* **B30**, 1971 (1984). See also G. Travaglini, P. Wachter, J. Marcus, and C. Schlenker, *Solid State Commun.* **37**, 599 (1981).
8. G. Grüner (private communication).
9. G. Grüner, A. Zawadowski, and P. M. Chaikin, *Phys. Rev. Lett.* **46**, 511 (1981).
10. J. Bardeen, *Phys. Rev. Lett.* **45**, 1978 (1980).
11. In a simple classical model of CDW transport which leads to Eq. (5) (ref. 9), the dc threshold field is related to the crossover frequency by $E_T = \omega_{CO} \frac{\lambda n e}{2\pi\sigma_0}$, with λ the CDW wavelength and n the CDW carrier concentration. This assumes a sinusoidal pinning potential. With $E_T = 500$ mV/cm, $\lambda = 30$ Å, and $n = 2 \times 10^{20}$ (see J. Dumas and C. Schlenker, *Solid State Commun.* **45**, 885 (1983)), and estimating $\sigma_0 = 4 \times 10^{30} \text{cm}^{-1}$, we find $\omega_{CO} = 1.414$ GHz.
12. Determined from data of Ref. 5.
13. Wei-Yu Wu, G. Mozurkewich, and G. Grüner, *Phys. Rev. Lett.* **52**, 2382 (1984).
14. M. Sato, H. Fujishita, and S. Hoshino, *Journal of Physics C16*, L877 (1983).
15. J. Dumas and C. Schlenker, *Proceedings of the International Symposium on Nonlinear Transport and Related Phenomena in Inorganic Quasi-one-Dimensional Conductors*, Sapporo, Japan (1983) p. 198.
16. R. J. Cava, R. M. Fleming, R. G. Dunn, E. A. Rietman, and L. F. Schneemeyer, *Phys. Rev. B* **30**, 7290 (1984).
17. G. Travaglini, I. Mörke, and P. Wachter, *Solid State Commun.* **45**, 289 (1983).